Praca oryginalna *Original paper*

Ultrasound image of the internal organs of cats with the effusive form of feline infectious peritonitis (FIP)

DOMINIKA SZULC[1], BANU DOKUZEYLÜL[2], MEHMET ERMAN OR[2], GÜLCE AYAŞ[2], PIOTR DĘBIAK[3], MARCIN KALINOWSKI[4], MAJA GRONOWSKA[4], ŁUKASZ ADASZEK[4]

[1]Vetiss Sp. z o. o., Lindleya 16, 02-013 Warsaw, Poland
[2]Department of Internal Medicine, Veterinary Faculty, Istanbul University-Cerrahpasa, 34320 Avcilar Campus, Avcilar, Istanbul, Türkiye
[3]Department and Clinic of Animal Surgery, Laboratory of Radiology and Ultrasonography, Faculty of Veterinary Medicine, University of Life Sciences in Lublin, Głęboka 30, 20-612 Lublin, Poland
[4]Department of Epizootiology and Clinic of Infectious Diseases, Faculty of Veterinary Medicine, University of Life Sciences in Lublin, Głęboka 30, 20-612 Lublin, Poland

Received 20.05.2025 *Accepted 15.07.2025*

Szulc D., Dokuzeylül B., Or M. E., Ayaş G., Dębiak P., Kalinowski M., Gronowska M., Adaszek Ł.

Ultrasound image of the internal organs of cats with the effusive form of feline infectious peritonitis (FIP)

Summary

Feline infectious peritonitis (FIP) is a widespread viral disease of cats and other Felidae. Diagnosis of the disease is difficult and relies on medical history, observed clinical signs, laboratory, molecular and imaging test results, and analysis of the fluid collected. The aim of the study was to perform an ultrasound examination to assess the internal organs of 127 cats with a molecularly confirmed effusive form of feline infectious peritonitis. Of all the animals qualified for the study, 13 cats (10%) had fluid accumulating in the pleural cavity, 26 (21%) individuals had fluid in both the pleural and the abdominal cavities, and 88 cats (69%) only had fluid in the abdominal cavity. The ultrasound examination revealed lesions in the organs, most frequently in the spleen, followed by the liver, gastrointestinal tract, lymph nodes, pancreas, kidneys and gallbladder. An ultrasound examination can significantly facilitate the diagnosis of FIP due to the development of ultrasound technology, improved image resolution, and a greater capacity to recognise small details in the internal organs. The limitation of the examination is, undoubtedly, the subjective analysis of images. It should be noted that further diagnosis of the disease following an ultrasound examination is advisable and that, based on an ultrasound image, it is not possible to diagnose FIP but only suspect it.

Keywords: feline infectious peritonitis, cats, ultrasound examination, PCR

Feline infectious peritonitis (FIP) is a widespread viral disease of cats and other Felidae. This highly fatal disease is caused by a form of the feline enteric coronavirus (FECV). The aetiological factor of feline infectious peritonitis (FIP) is a virus belonging to the order *Nidovirales*, family *Coronaviridae*, subfamily *Coronavirinae*, and the genus alpha (α)-CoV. It is a single-stranded RNA virus, positively polarised, whose genome is a strand with a size of 27-32 kb (5, 6). Numerous mutations in the FCoV genome play a significant role in the pathogenesis of feline infectious peritonitis. Mutations within the gene encoding the structural protein S at positions 23531 and 23537, resulting in the exchange of methionine for leucine at position 1058 (M1058L), and of serine for alanine at position 1060 (S1060A), contribute to the formation of FIPogenic FCoV strains (3, 11).

Until now, the disease has mainly been noted in young kittens aged between a few months and 2 years. Currently, it is being diagnosed in individuals of all ages, even over the age of 12. Two forms of the disease are distinguished: dry – involving the formation of granulomatous lesions in the organs, and wet – an acute form involving the formation of effusion in the body cavities (16).

The development of FIP is affected by numerous factors, including the presence of many coronavirus mutants in monocytes/macrophages and the state of immunosuppression. A weak cellular response to the presence of the virus, with an intense B-cell response, is associated with the development of the effusive form of FIP, while a stronger T-cell response is observed in individuals with the dry form of FIP (14).

Diagnosing FIP poses a challenge for veterinary surgeons. The diagnosis should rely on a comprehensive analysis of the cat's examination results, including medical history, clinical signs, blood tests and serological and molecular test results.

For patients with FIP, an ultrasound examination is part of the diagnostic procedure. The ultrasound image of the internal organs in cats affected by feline infectious peritonitis can be sufficiently characteristic to enable the suspicion of this disease, which undoubtedly accelerates the diagnostic process and enables an earlier onset of the therapy (7, 8).

The aim of the study was to perform an ultrasound examination to assess the internal organs of cats with molecularly confirmed feline infectious peritonitis.

Material and methods

Animals used in the study. The study was conducted on 127 cats (58 females, 69 males), aged between 3 months and 16 years and 8 months, patients of veterinary clinics and practices from all over Poland, which were suspected of having an effusive form of feline infectious peritonitis based on the results of clinical, haematological, molecular and ultrasound examinations. The animals were qualified for the study based on the presence of fluid in the abdominal and/or thoracic cavity and a positive PCR test result for the presence of the coronavirus and the presence of mutations within its genome.

Molecular studies. Total RNA isolation from the abdominal/thoracic fluid was performed using the Total RNA Mini kit (A&A Biotechnology, Gdańsk, Poland) according to the procedure provided by the manufacturer.

The formation of cDNA in the process of reverse transcription: in order to obtain cDNA, the isolated RNA was subjected to the reverse transcription reaction. The reactive mixture consisted of two mixtures (I and II).

The composition of the first mixture was as follows: 9.5 µL of water, 5.0 µL of isolated total RNA and 1.0 µL of Hexamer p(dN)6 (Invitrogen, USA). The second reaction mixture consisted of: 5.0 µL of Reverse transcriptase-specific buffer (Fermentas, Lithuania), 2.5 µL of dNTP (2 mM) (Fermentas, Lithuania), 1.0 µL of RNase inhibitor (10 u/µL) (Fermentas, Lithuania) and 1.0 µL of Reverse transcriptase (200 u/µL) (Fermentas, Lithuania).

Mixture I was incubated in a water bath for 5 minutes at 65°C and then placed on ice for another 5 minutes. Next, 9.5 µL of mixture II was added to the test tubes containing mixture I and centrifuged at 5000 rpm for 30 seconds. The cDNA synthesis was performed at 42°C for 60 minutes in a Corbett thermal cycler. The reaction mixture was incubated at 94°C for 5 minutes (1).

Real-Time PCR reaction. A fragment of the S gene was amplified using Real-Time PCR. The quantitative analysis of the studied gene expression was performed using 2 µL of the matrix containing 200 ng of cDNA. The real-time polymerase chain reaction was carried out in 20 µL thin-walled tubes using the DyNAmo HS SYBR Green qPCR Kit (Finnzymes, Finland), enabling a highly specific qualitative and quantitative reaction. PCR was performed by using specific primers (sense 5'-CAATATTACAATGGCATAATGG-3', antisense 5'-CCCTCGAGTCCCGCAGAAACCATACCTA-3') for the first reaction and specific primers (sense 5'-GGCATAATGGTTTTACCTGGTG-3', antisense 5'-TAATTAAGCCTCGCCTGCACTT-3') for the second reaction. PCR cycling conditions were 30 cycles at 94°C for 60 s, at 50°C for 30 s, and at 72°C for 1 min plus a 7-min extension at 72°C at the end of the reaction. Primer pairs were expected to generate a 598-bp product covering nucleotides 23442-24040 for the first PCR run and a 142-bp product covering nucleotides 23451-23593 (which includes deviant position 23531 – (i.e., mutation M1058L) for the second run for the first PCR (1).

The 20 µL volume of the initial reaction mixture contained: 2 µL of DNA matrix, 7.2 µL of water, 0.4 µL of each primer (final concentration 50 pM), 10 µL of Master Mix containing the hot start version of the modified Tbr polymerase (Thermus brockianus), buffer for Tbr polymerase, dNTP, $MgCl_2$ and SYBR Green 1 intercalating dye.

Reactions were performed using a Rotor-Gene3000 thermal cycler, Corbett Research (Australia). The Ct value of the Real-Time PCR products generated on the cDNA matrix was determined for each reaction (the number of amplification cycles after which the fluorescence intensity of the resulting product exceeded the background fluorescence). To confirm the amplification specificity, the melting point of the PCR products was determined by gradually increasing the temperature of the reaction mixture from 50°C to 95°C while continuously measuring fluorescence (1).

Ultrasound examination. The patients were examined in the dorsal and lateral positions, and in the case of a very large amount of fluid in the abdominal cavity, also in the standing position. The examination was performed with an Esaote Mylab Omega apparatus, using a 3-11 MHz microconvex probe and a 4-15 MHz linear probe, as well as GE Vivid iq, 4-10 MHz microconvex transducers and a 4-13 MHz linear transducer, and GE Versana Active, 4-10 MHz microconvex transducers and a 4-13 MHz linear transducer.

Before the examination, the patient's abdomen was shaved, the skin was disinfected with alcohol, and gel was applied. During the thoracic ultrasound, there was no need to shave the patient, and alcohol together with gel were used.

The abdominal organs were visualised in a longitudinal and/or transverse section, depending on the patient's condition. The study measured the altered organs, including the size of the spleen in a longitudinal section in the area of the hilus of the spleen, the height of the left pancreatic lobe in the area of the stomach and spleen, and the height of the mesenteric lymph nodes in a longitudinal section. Assessments were made of the echogenicity and echostructure of the liver, spleen, and left pancreatic lobe, as well as the lymph nodes (without assessed margination), and other altered organs in compare with other abdominal organs. The presence of te fluid in abdominal cavity was also analyzed.

During the thoracic ultrasound, attention was paid to the presence, echogenicity and amount of fluid in the thorax, the presence of atelectatic lungs, and the presence of B-line artefacts arising from the pleura. B-lines – vertical artifacts originating from the pleural line and moving with lung sliding; and C-lines – artifacts associated with focal lung lesions and consolidations. In the effusive form of FIP, the presence of fluid in the abdominal and/or thoracic cavity was assessed, along with its echogenicity.

The amount of fluid was classified as:

a) small – when fluid was present only beneath the pleura;

b) moderate – when visible only retrocardially in the cardiophrenic angle or cranially in the precordial area;

c) large – when present throughout the entire thoracic cavity – precordially, in the mediastinum, and retrocardially.

Results and discussion

The presence of the genetic material of the mutant feline coronavirus was demonstrated in the fluid collected from 127 cats constituting the study group. The following range of the ct value 20-24, for individual samples was observed. By assessing the melting point of the obtained amplicons, it can be concluded that the conducted reactions were characterised by high specificity, which was confirmed by the similar melting point value of the PCR products, i.e., 81.0-81.2°C (in the case of enteric coronavirus, this value is lower, at about 83.3-83.5°C) (1).

The most common clinical signs observed in the cats under study included apathy (79.5%; 101/127) and weakness, manifested by the unwillingness of young cats to play (66.1%; 84/127), loss of appetite (64.6%; 82/127), abdominal distension 60.6%; 77/127), which was particularly noticeable in young cats, and misinterpreted as helminthiasis. The least common symptoms noted included diarrhoea (6.3%; 8/127) and vomiting (3.9%; 5/127).

An ultrasound examination of cats with diagnosed FIP determined the nature of the fluid, as well as its location (abdominal and/or pleural cavity). In 13 cats (10%), fluid accumulated in the pleural cavity, 26 individuals (21%) had fluid in both the pleural and the abdominal cavities, and 88 cats (69%) only had fluid in the abdominal cavity.

Aechogenic fluid in the abdominal cavity was noticeable in 51 cats (58%), whereas echogenic fluid was noticeable in 37 animals (29%) (Figs. 1A, B). Omentum bands, mesentery and mesenteric fat – convoluted, markedly hyperechogenic, surrounding the organs, were noted in 111 animals under study (87%).

Reactive peritoneum fat and free fluid in abdominal cavity was visible on ultrasound in 111 affected cats (87%). Notably, when there were medium to large volumes of fluid, the peritoneal fat appeared thickened and irregular (Figs. 2A, B). Additionally, as the duration of the disease increased, loosely suspended fibrin strands and hyperechoic inclusions became more common on

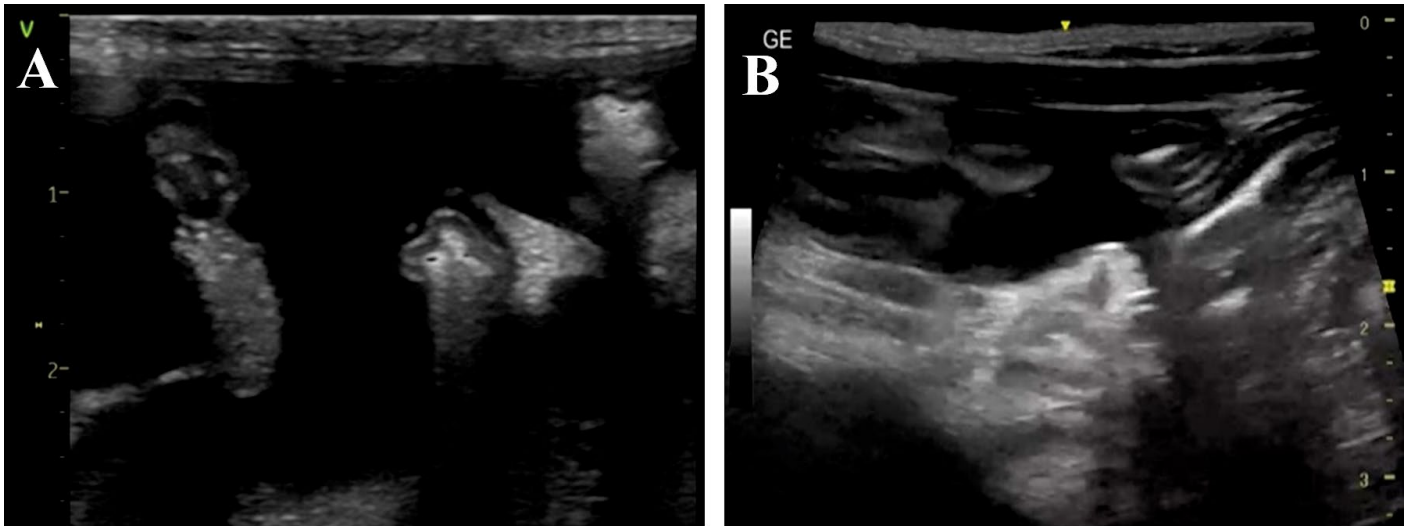

Fig. 1. A, B – Aechogenic fluid in the abdominal cavity between the small intestine loops

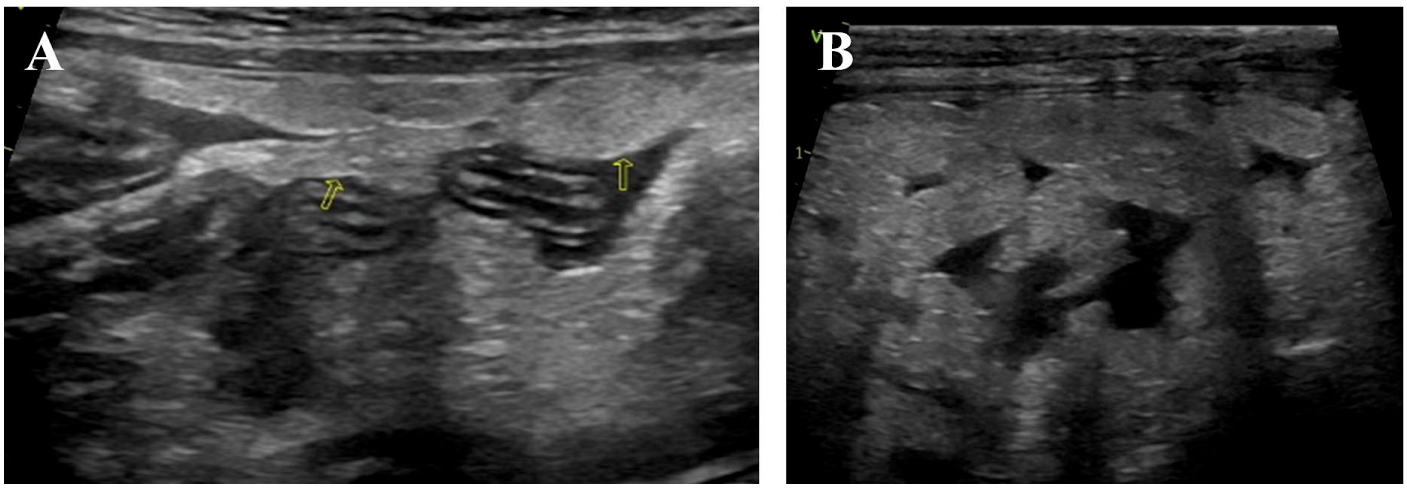

Fig. 2. A – Hyperechogenic peritoneal reaction indicated by arrows – in the area of the irregular and thickened mesentery and peritoneal fat between the loops of the small intestine; B – Hyperechogenic, irregular, thickened, with elevated echogenicity

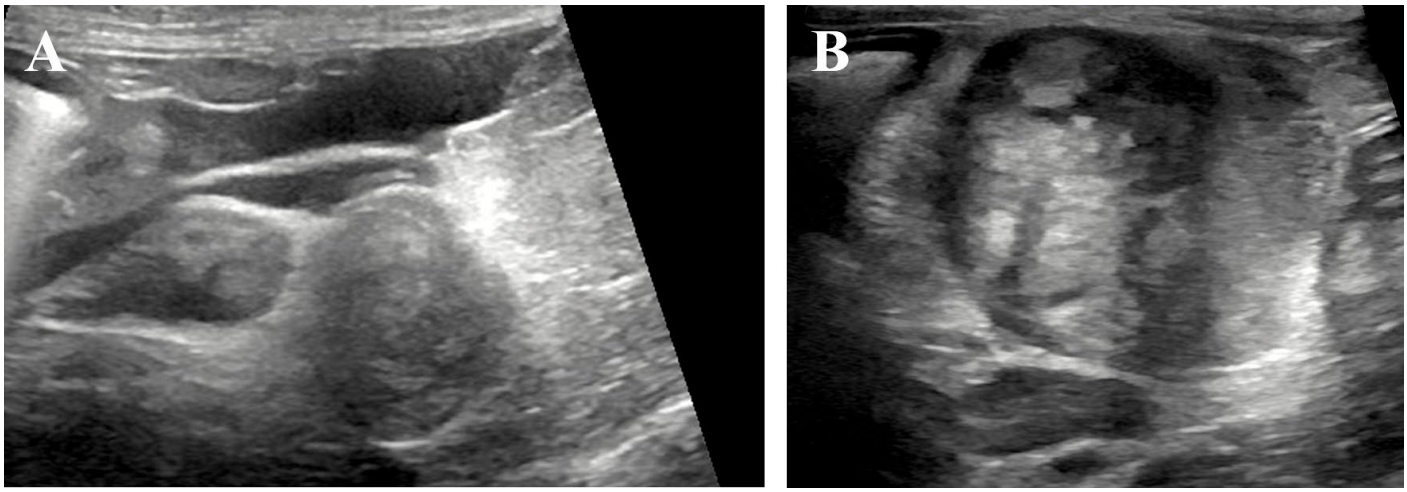

Fig. 3. A – The mesenteric lymph nodes surrounded by a hyperechogenic inflammatory reaction; B – A markedly enlarged, heterogenous mesenteric lymph node between the loops of small intestines

the peritoneal surface. In cases where fluid was only visible in the pleural cavity, the peritoneum fat showed no increased echogenicity or in its echogenicity there was slight increase.

The mesenteric lymph nodes were considered enlarged if their size exceeded 5 mm. Heterogeneous lymph nodes were observed in 75 cats (59%). In 11 animals (8.7%), the lymph nodes were non-enlarged and homogeneous, while in 54 animals (42.5%), they were non-enlarged and heterogeneous, with a normal hyperechoic hilus (Figs. 3A, B).

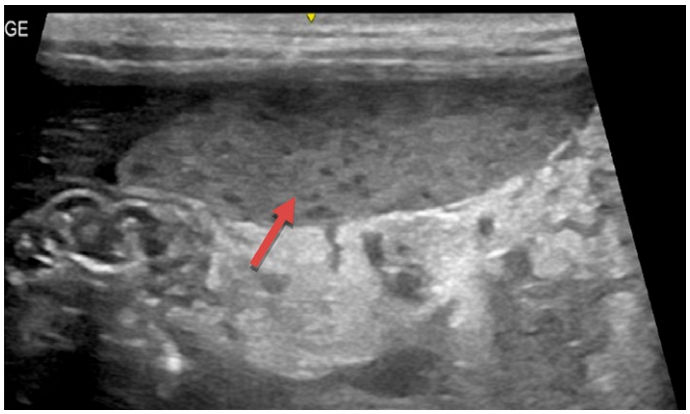

Fig. 4. Spleen parenchyma (indicated by the arrow) surrounded by reactive, hyperechogenic fat

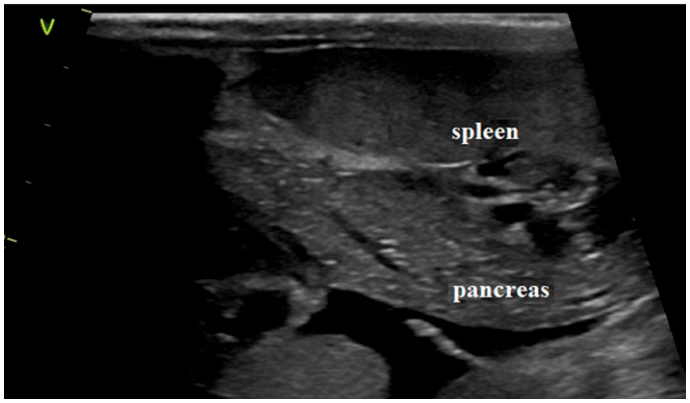

Fig. 5. The pancreas – thickened, irregular left lobe located along the spleen

The spleen, a lymphatic organ, most often showed interstitial lesions diffusely scattered, fairly well-demarcated hypoechoic foci, and was enlarged (> 1 cm at the body). This condition was observed in 84 cats with FIP (66.1%) (Fig. 4).

For the pancreas, a size standard of up to 6 mm was adopted for the left lobe (4). The echogenicity of the organ is considered normal when it is similar to that of the liver. In 68 cats under study (53.5%), the pancreas was enlarged and irregular at the edges (the left lobe of over 6 mm), with the echogenicity in relation to the surrounding tissues markedly reduced (Fig. 5).

Non-enlarged kidneys (< 4.5 cm in length, normoechogenic) were noted in 67 animals under study (52.6%). Kidneys with reduced corticomedullar differentiation were visualised in 19 individuals, whereas kidneys with the hyperechogenic medullary rim sign were visualised in 19 cats. In two cases, a subcapsular hypoechogenic 'halo effect' was visualised. In one cat, showed irregular contour of the kidneys, which were probably granulomas (Figs. 6A, B and Fig. 7).

In 80 cats (63%) with confirmed feline infectious peritonitis, the liver was enlarged on the ultrasound. The left lobe clearly extended beyond the edge of the stomach, was rounded and reached beyond the last rib (Figs. 8A, B). In 30 cats (23.6%), the gallbladder contents, which are physiologically aechogenic, were found to contain hyperechogenic biliary thickening with mild sludge formation. In some animals, thickening of the gallbladder wall over 1 mm was demonstrated.

The ultrasound examination of the gastrointestinal tract in 79 affected cats (62.2%) revealed lesions in the gastrointestinal tract associated with the presence of an asymmetric additional hyperechogenic layer within the mucosal layer of the small intestine loop, gastrointestinal atony, slight thickening of the muscular layer (over 1.2 mm), corrugation of the small intestinal wall, and thickening of the caecal wall (over 1.5 mm) with a decrease in its echogenicity (Figs. 9A, B, C, D, E).

A thoracic ultrasound revealed lesions in 38 cases (29.9%). Medium-to-large amounts of fluid in the

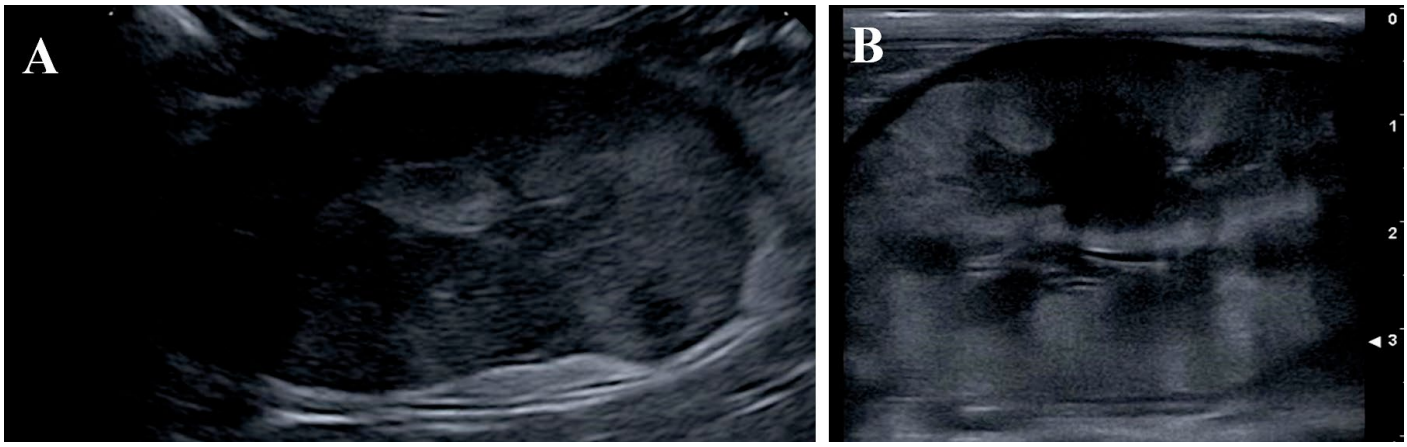

Fig. 6. A – Renal alteration in a 12-year-old female cat with FIP. Markedly blurred corticomedullar differentiation, strongly irregular edges of the kidney, with circular interstitial lesions in the cortical layer causing deformation of the organ's edges; B – An image of the kidney in another cat – enlarged kidney with unclear corticomedullar differentiation, with elevated echogenicity of the cortical layer, subcapsular halo effect. The HP test result confirmed the infiltration of inflammatory cells with foci of necrosis

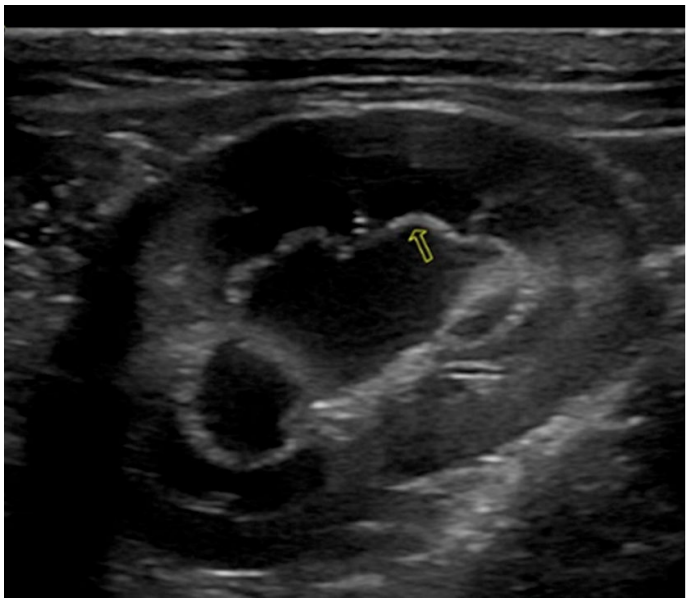

Fig. 7. Hyperechogenic medullary rim sign in a cat with FIP (indicated by the arrow)

pleural cavity were visible in 26 cats (21%), along with lesions within the area of sternal lymph nodes, which were enlarged (over 5 mm), heterogenous, with multiple small hypoechogenic foci (indicating reactivity) (10), rounded. In 7 cats, an irregular pleural edge and B-line and C-line artefacts arising from it were found.

FIP is a disease that affects cats and can develop a broad spectrum of clinical symptoms (2, 12). Therefore, its differential diagnosis should take into account, *inter alia*, bacterial peritonitis (with bacteria then present in the fluid), lymphoma (biopsy is an additional test to detect the presence of neoplastic cells), toxoplasmosis (blood and stool tests enable the identification of tachyzoites), pancreatitis (diagnosed based on the examination of the specific pancreatic lipase concentration), and cholangitis (hepatic parameters increase more than in FIP) (13, 15).

FIP diagnosis faces many problems, mostly due to the inability to distinguish between enteric coronavirus strains from those causing FIP. Haematological and biochemical tests cannot clearly confirm the form of

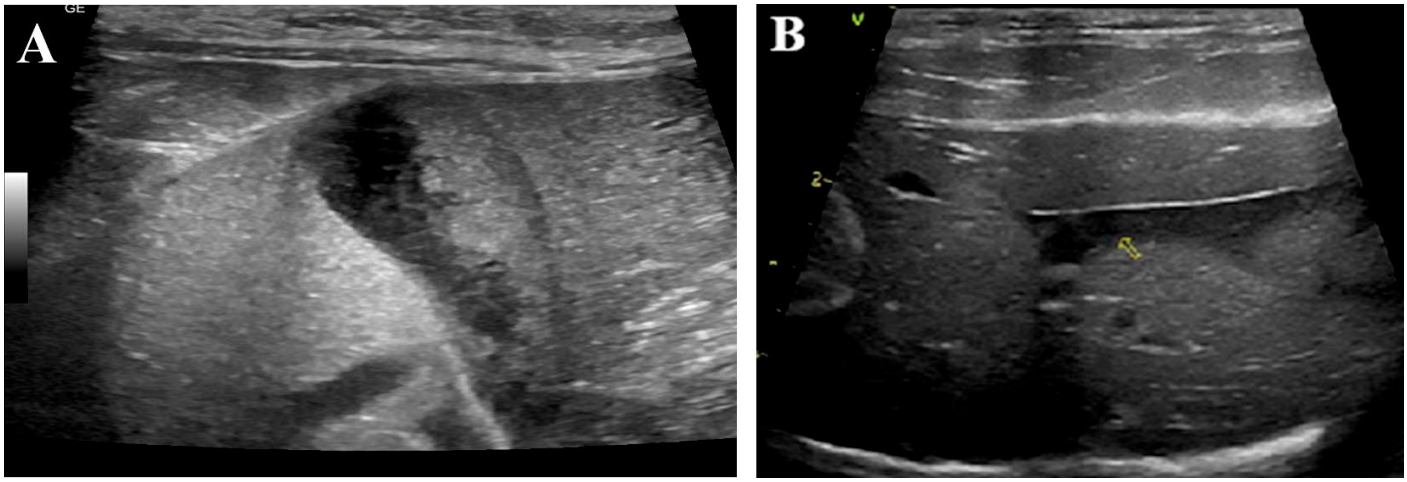

Fig. 8. A – Condensed bile in the gallbladder lumen, indicated by the yellow arrow; B – Enlarged liver with fluid between the hepatic lobes. Rounded edges of the liver lobes, the left lobe of the liver extending beyond the stomach and passing to the left splenic side. Reduced echogenicity of the liver parenchyma

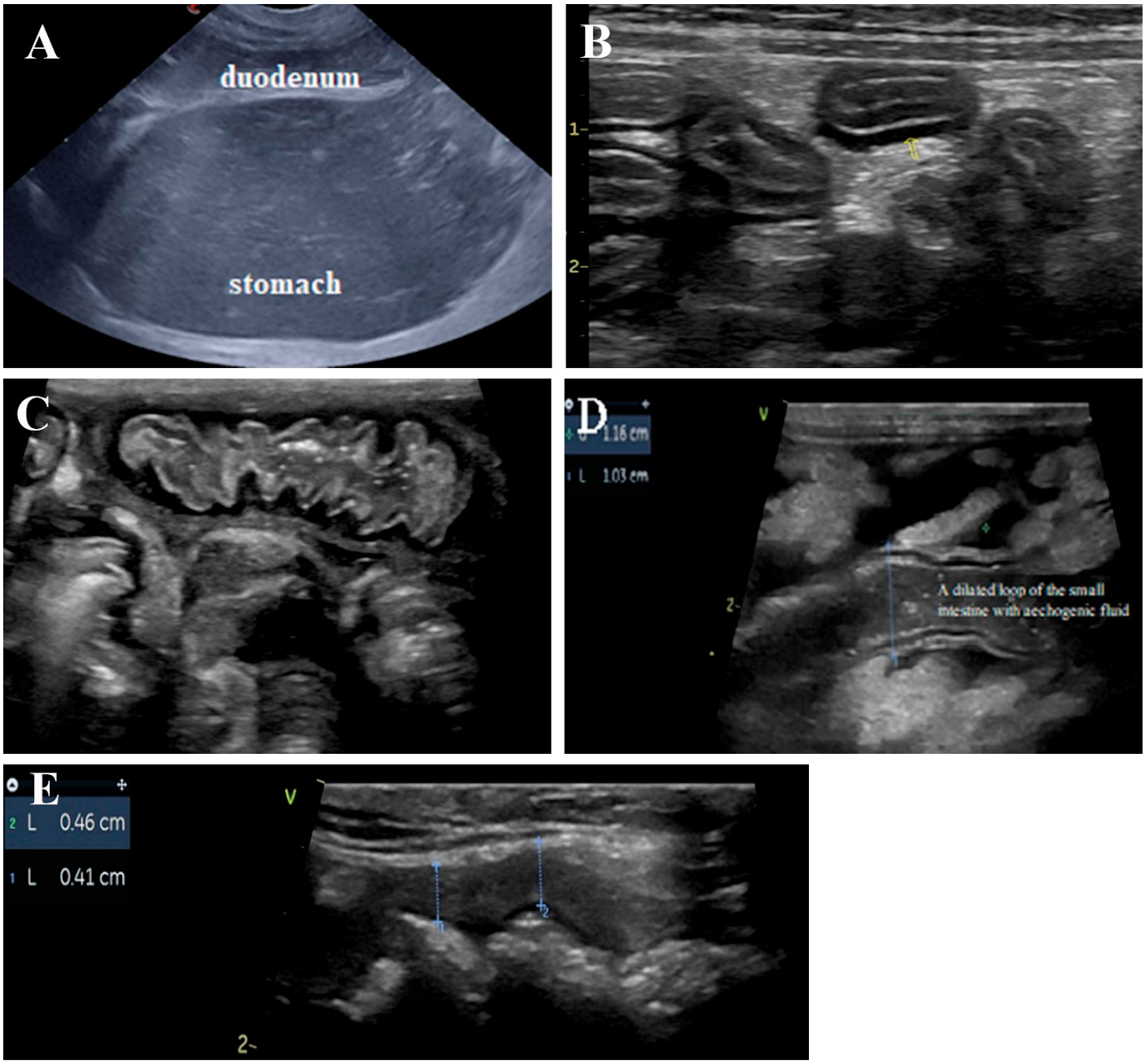

Fig. 9. A – High-grade gastric dilatation, with fluid content retention. In addition, the duodenum has changed its location. In the intestinal lumen, fluid echogenic content is visible, with lumen dilatation; B – Thickening of the muscular layer of the small intestinal wall in cases of FIP, observed from a slight to a significant degree; C – Wrinkling of the intestinal wall; D – A dilated loop of the small intestine between the orientation markers, with aechogenic fluid visible between the intestines. Dilated duodenum with stagnated digestive contents, retention, and dilatation of the loop with the lamination preserved; E – Altered, thickened colon wall, with unclear differentiation of the wall lamination

FIP (9, 12). This disease is practically always associated with neutrophilia (often with a shift to the left). About half of the cats with FIP suffer from anaemia and/or lymphopenia, and one in three has microcytosis (< MCV). In biochemical tests, nearly 90% of cats with FIP have a hypergammaglobulinemia and/or serum albumin-to-globulin ratio < 0.8. Of all the above non-specific changes in laboratory test results, an albumin-to-globulin ratio decrease is relatively often associated with FIP and rarely with other diseases.

The detection of this virus in the fluid collected from body cavities strongly suggests the presence of FIP. If a non-effusive form is suspected, blood is usually the only test material available. However, a positive RT-PCR result from blood does not necessarily confirm FIP because, as mentioned above, the enteric biotype may also be found in the blood. This diagnostic breakthrough was possible thanks to the opportunity to differentiate coronavirus biotypes based on the presence of the M1058L or S1060A mutations (3). The detection of one of the two above-described mutations in the peritoneal fluid, the anterior chamber, the cerebrospinal fluid or the bioptate is sometimes regarded as a definitive confirmation of FIP. In the authors' own studies, the presence of

FCoV with the M1058L mutation was confirmed in the abdominal fluid of all the cats in the study group. This mutation results from the replacement of adenine at position 23531 of the FCoV S protein gene with thymine or cytosine, which in turn translates into a replacement of methionine to leucine at position 1058 of the amino acid sequence of the protein. The nucleotide replacement at position 23531 also results in the higher melting point of amplicons from FIPV strains compared to FCoV strains, and therefore, they can be differentiated using the real-time HRM Sybr Green technique (3).

The presence of fluid in the abdominal cavity is one of the typical FIP symptoms, which raises suspicion of the disease (9). It should be noted, however, that the fluid in feline body cavities can also accumulate in the course of other nosological units, e.g. hepatitis, lymphoma, circulatory failure or bacterial infections. Such disturbances should be considered in a differential diagnosis of feline infectious peritonitis (17). The fluid typical of FIP is yellow, sticky and viscous. There are cases, however, where the fluid is atypical, blood-stained, and watery (15). The authors' study demonstrated that the severity of peritoneal tissue reaction detected by ultrasound was directly proportional to its volume. Similar observations were made by Müller et al. (8), who additionally found that the lesions affecting the peritoneum are secondary to granulomatous and necrotic processes occurring within the abdominal organs in the course of the disease.

In cats with the effusive form of FIP, the organ most commonly showing changes on ultrasound was the spleen, affected in 66% of cases in the studied group. This rate appears high, especially considering that previous studies reported spleen size changes in only 12% of cats with FIP (7, 8).

As far as kidneys are concerned, the changes in ultrasound scans observed in the authors' own study are consistent with the literature data, according to which cats with FIP most often show renomegaly, irregular kidney contour (7, 8).

In 88 cats, low echogenicity of the liver was observed, which could have been the result of contrast with reactive peritoneum. This organ was hyperechogenic in only six cats. An elevation of the echogenicity of the liver parenchyma is found in cases of vacuolar degeneration (steatosis), chronic inflammatory processes, fibrosis or lymphoma. According to some authors, elevated echogenicity of the parenchyma may be associated with fatty liver in cats with FIP, although, depending on the degree of steatosis, changes in ultrasound may not be visible (8).

Overall, changes in the ultrasound image of the gastrointestinal tract occurred in 62% of cats with FIP. Until now, changes in the gastrointestinal tract have not been frequently noted (they have been found in approximately 13% of the cats under study). In later studies, the frequency of their diagnosis was similar to that found in the authors' observations (7, 8). The most common finding was wall thickening, which should be differentiated from neoplasia, especially in older cats.

Thanks to the development of ultrasound technology, improved image resolution, and a greater capacity to recognise small details in the internal organs, an ultrasound examination can significantly facilitate the diagnosis of FIP. The limitation of the examination is, undoubtedly, the subjective analysis of images. It should be noted that further diagnosis of the disease following an ultrasound examination is advisable and that, based on an ultrasound image, it is not possible to diagnose FIP but only suspect it. The lesions in the liver, spleen or other organs, as detected by ultrasound, are not typical enough to diagnose FIP based on them. The likelihood of the disease increases when an ultrasound examination detects fluid, enlarged mesenteric lymph nodes, reactive splenic parenchyma, or irregular kidney images (7, 8).

References

1. *Adaszek Ł., Kalinowski M., Rutkowska-Szulczyk M., Mazurek Ł., Szulc D., Staniec M., Pietras-Ożga D., Michalak K., Buczek K., Winiarczyk S.*: Comparison of the sensitivity of rapid tests FCoV Ab (Vet Expert) and PCR in the diagnosis of feline infectious peritonitis (FIP) in cats with the effusive form of the disease. Med. Weter. 2023, 79, 130-133.
2. *Beatty J., Barrs V.*: Pleural effusion in the cat: a practical approach to determining aetiology. J. Feline Med. Surg. 2010, 12, 693-707.
3. *Chang H. W., Egberink H. F., Halpin R., Spiro D. J., Rottier P. J.*: Spike protein fusion peptide and feline coronavirus virulence. Emerg. Infect. Dis. 2012, 18, 1089-1095.
4. *Etue S. M., Penninck D. G., Labato M. A., et al.*: Ultrasonography of the normal feline pancreas and associated anatomical landmarks: a prospective study of 20 cats. Vet. Radiol. Ultrasound 2001, 42 (4), 330-336.
5. *Gorbalenya A. E., Enjuanes L., Ziebuhr J., Snijder E. J.*: Nidovirales: evolving the largest RNA virus genome. Virus Res. 2006, 117, 17-37.
6. *Lewis C. S., Porte E., Matthews D., Kipar A., Tasker S., Helps C. R., Siddell S. G.*: Genotyping coronaviruses associated with feline infectious peritonitis. J. Gen. Virol. 2015, 96, 1358-1368.
7. *Lewis K. M., O'Brien R. T.*: Abdominal ultrasonographic findings associated with feline infectious peritonitis: a retrospective review of 16 cases. J. Am. Anim. Hosp. Assoc. 2010, 46, 152-160.
8. *Müller T. R., Penninck D. G., Webster C. R., Conrado F. O.*: Abdominal ultrasonographic findings of cats with feline infectious peritonitis: an update. J. Feline Med. Surg. 2023, 25, 1098612X231216000.
9. *Pedersen N. C.*: An update on feline infectious peritonitis: diagnostics and therapeutics. Vet. J. 2014, 201, 133-141.
10. *Penninck D. G., d'Anjou M.*: Atlas of Small Animal Ultrasonography. 2nd ed. Ames: Wiley Blackwell 2015.
11. *Porter E., Tasker S., Day M. J., Harley R., Kipar A., Siddell S. G., Helps C. R.*: Amino acid changes in the spike protein of feline coronavirus correlate with systemic spread of virus from the intestine and not with feline infectious peritonitis. Vet. Res. 2014, 45, 49.
12. *Riemer F., Kuehner K. A., Ritz S., Sauter-Louis C., Hartmann K.*: Clinical and laboratory features of cats with feline infectious peritonitis – a retrospective study of 231 confirmed cases (2000-2010). J. Feline Med. Surg. 2016, 18, 348-356.
13. *Tasker S.*: Diagnosis of feline infectious peritonitis: update on evidence supporting available tests. J. Feline Med. Surg. 2018, 20, 228-243.
14. *Tekes G., Thiel H. J.*: Feline coronaviruses: Pathogenesis of feline infectious peritonitis. Adv. Virus Res. 2016, 96, 193-218.
15. *Thayer V., Gogolski S., Felten S., Hartmann K., Kennedy M., Olah G. A.*: AAFP/EveryCat feline infectious peritonitis diagnosis guidelines. J. Feline Med. Surg. 2022, 24, 905-933.
16. *Yin Y., Li T., Wang C., Liu X., Ouyang H., Ji W., Liu J., Liao X., Li J., Hu C.*: A retrospective study of clinical and laboratory features and treatment on cats highly suspected of feline infectious peritonitis in Wuhan, China. Sci. Rep. 2021, 11, 5208.
17. *Zwicklbauer K., Bergmann M., Alberer M., Both U. von, Hartmann K.*: Feline infectious peritonitis – a current overview. Tierarztl. Prax. Ausg. K Kleintiere Heimtiere 2025, 53, 96-102.

Corresponding author: Marcin Kalinowski, DVM, PhD, Głęboka 30, 20-612 Lublin, Poland; e-mail: marcin.kalinowski@up.lublin.pl